HHS Public Access

Author manuscript

Matrix Biol. Author manuscript; available in PMC 2017 May 01.

Published in final edited form as:

Matrix Biol. 2016 ; 52-54: 339–354. doi:10.1016/j.matbio.2016.03.001.

Osteophyte formation and matrix mineralization in a TMJ osteoarthritis mouse model are associated with ectopic hedgehog signaling

Till E. Bechtold[1,3], **Cheri Saunders**[1], **Rebekah S. Decker**[1], **Hyo-Bin Um**[1], **Naiga Cottingham**[1], **Imad Salhab**[2], **Naito Kurio**[2], **Paul C. Billings**[1], **Maurizio Pacifici**[1], **Hyun-Duck Nah**[2], and **Eiki Koyama**[1]

[1]Division of Orthopaedic Surgery, The Children's Hospital of Philadelphia, Philadelphia, PA 19104

[2]Division of Plastic and Reconstructive Surgery, Department of Surgery, The Children's Hospital of Philadelphia, Philadelphia, PA 19104

[3]Department of Orthodontics and Orofacial Orthopaedics, Center of Dentistry, Oral Medicine and Maxillofacial Surgery, University Hospital Tuebingen, D-72076 Tuebingen, Germany

Abstract

The temporomandibular joint (TMJ) is a diarthrodial joint that relies on lubricants for frictionless movement and long-term function. It remains unclear what temporal and causal relationships may exist between compromised lubrication and onset and progression of TMJ disease. Here we report that *Proteoglycan 4* (*Prg4)*-null TMJs exhibit irreversible osteoarthritis-like changes over time and are linked to formation of ectopic mineralized tissues and osteophytes in articular disc, mandibular condyle and glenoid fossa. In the presumptive layer of mutant glenoid fossa's articulating surface, numerous chondrogenic cells and/or chondrocytes emerged ectopically within the *type I collagen*-expressing cell population, underwent endochondral bone formation accompanied by enhanced *Ihh* expression, became entrapped into temporal bone mineralized matrix, and thereby elicited excessive chondroid bone formation. As the osteophytes grew, the roof of the glenoid fossa/eminence became significantly thicker and flatter, resulting in loss of its characteristic concave shape for accommodation of condyle and disc. Concurrently, the condyles became flatter and larger and exhibited ectopic bone along their neck, likely supporting the enlarged condylar heads. Articular discs lost their concave configuration, and ectopic cartilage developed and articulated with osteophytes. In glenoid fossa cells in culture, hedgehog signaling stimulated chondrocyte maturation and mineralization including alkaline phosphatase, while treatment with hedgehog inhibitor HhAntag prevented such maturation process. In sum, our data indicate that *Prg4* is needed for TMJ integrity and long-term postnatal function. In its absence, progenitor cells near

Corresponding author: Eiki Koyama, Division of Orthopaedic Surgery, The Children's Hospital of Philadelphia, 3615 Civic Center Boulevard, ARC Suite 902, Philadelphia, PA 19104, USA, 267-425-2074 (phone), 267-426-7814 (fax), ; Email: koyamae@email.chop.edu.

The authors declare no potential conflicts of interest with respect to the authorship and/or publication of this article.

presumptive articular layer and disc undergo ectopic chondrogenesis and generate ectopic cartilage, possibly driven by aberrant activation of Hh signaling. The data suggest also that the *Prg4*-null mice represent a useful model to study TMJ osteoarthritis-like degeneration and clarify its pathogenesis.

Keywords

TMJ; osteophyte; heterotopic cartilage; Prg4; lubricin; Ihh

INTRODUCTION

The TMJ is a diarthrodial joint that permits the articulation of mandibular condyle and glenoid fossa /articular eminence in the temporal bone. The TMJ contains a characteristic and unique articular disc that divides the articular cavity into upper and lower joint cavity compartments. The synovial cells, disc lining cells and superficial cells of articular cartilage all produce and secrete important constituents of the synovial fluid (Nitzan, 2003; Scrivani et al., 2008). Synovial fluid is found to have two main functions: 1) to aid in nutrition of articular cartilage and synovium; and 2) to reduce friction and facilitate movement between the articulating joint components (Jay et al., 2000; Smith, 2011). Since the TMJ's function involves comprehensive motions including rotation and translation, lubrication of articulating surfaces is critically vital and if altered, may contribute to TMJ dysfunction, leading to degenerative changes of structural components and progressive loss of function (Nitzan, 2003; Tanaka et al., 2008a; Tanaka et al., 2008b).

Unlike synovial joints in limbs and other sites that contain hyaline cartilage (Pacifici et al., 2005), the articular cartilage of mandibular condyle and glenoid fossa/eminence is composed of a fibrocartilaginous tissue that provides adaptive capacity to mechanical stress and can even undergo remodeling if mechanical stresses exceed the host's adaptive capacity (Arnett et al., 1996; Tanaka et al., 2008a). TMJ osteoarthritis (TMJ OA) is characterized primarily by degradation of articular cartilage and bone in mandibular condyles and glenoid fossa/eminence and often results in orofacial pain and reduced jaw function (Hunter and Kalathingal, 2013; Shintaku et al., 2006). Pathological changes associated with TMJ OA commonly manifest themselves in the form of: flattening of condyle and eminence; erosion, sclerosis and increased thickness of the glenoid fossa; and even osteophyte formation (Hussain et al., 2008; Zarb and Carlsson, 1999). Osteophytes, referred to as bony spurs, are one of the radiographic hallmarks of TMJ degenerative joint disease and represent a late stage of the disease resulting from the host's adaptive responses (Hunter and Kalathingal, 2013; Hussain et al., 2008). Compared to OA synovial joints in appendicular skeletal elements, osteophyte formation in TMJ OA is relatively rare; once developed however, the osteophytes can eventually compromise TMJ function (Hunter and Kalathingal, 2013; Rando and Waldron, 2012).

The *Proteoglycan 4* (*Prg4*) gene encodes lubricin, a mucin-like molecule that plays essential biological roles in boundary lubrication and joint movement and protects articular cartilage from friction-induced damage (Flannery et al., 2009; Gleghorn et al., 2009; Schmidt et al.,

2007). *PRG4* mutations in humans are responsible for camptodactyly-arthropathy-coxa vara-pericarditis syndrome (CACP), an autosomal recessive disorder (Marcelino et al., 1999). Synovial joints and associated tissues in CACP patients appear normal at birth, but eventually undergo failure associated with non-inflammatory hyperplasia and fibrosis of the synovial membrane, articular cartilage fibrillation, flexion deformity in the fingers, intervertebral disc damage and abnormal bone remodeling, leading to joint failure (Marcelino et al., 1999). In synovial joints, *Prg4* is expressed by synoviocytes, synovial membrane and superficial articular cartilage cells (Flannery et al., 1999; Jay et al., 2001). Changes in *Prg4* expression and lubricin levels have been reported in a mouse OA injury model and in humans with OA and rheumatoid arthritis (Elsaid et al., 2008; Elsaid et al., 2005; Rhee et al., 2005). Genetically engineered mice lacking *Prg4* recapitulate some of joint phenotypes observed in CACP patients, including synovial membrane hyperplasia and articular cartilage deterioration (Rhee et al., 2005). Notably, *Prg4*-null mice also displayed characteristic features of degenerative changes in TMJs including articular surface deterioration, loss of disc concave-convex morphology, synovial membrane hyperplasia and protein deposition. (Hill et al., 2014; Koyama et al., 2014). We also reported that *Prg4*-null mice displayed increased levels of chondrogenesis and ectopic cartilage formation within TMJ components (Bechtold et al., 2015; Koyama et al., 2014), but the cellular, signaling and molecular mechanisms underling such potentially important pathogenic transformation remains unclear.

Indian hedgehog (Ihh) signaling has well-established roles in endochondral bone formation by regulating chondrocyte proliferation and differentiation rate during skeletal development and growth, including in the TMJ (Maeda et al., 2007; Ochiai et al., 2010; Shibukawa et al., 2007). Recent studies revealed that hedgehog signaling is also involved in cartilage degradation and subsequent OA development and progression in a mouse injury model and in human patients (Alman, 2015; Lin et al., 2009). More recently, we demonstrated the stimulatory effects of hedgehog (Hh) signaling on early chondrogenesis and proteoglycan synthesis in primary limb bud mesenchymal cells in vitro (Mundy et al., 2015). Thus, we hypothesized that Hh signaling could be involved in ectopic chondrocyte differentiation and subsequent osteophyte formation observed in *Prg4*-null TMJs. Here, we investigated the major steps of osteophyte formation in glenoid fossa/eminence in *Prg4*-null mice. We found that numerous *Ihh*-expressing chondrocytic cells developed within the presumptive articular mesenchymal layer, underwent hypertrophy and subsequently formed osteophytes near the glenoid fossa. Using primary cells from glenoid fossa in vitro, we found that treatment with recombinant human Sonic hedgehog promoted chondrocyte differentiation, maturation and mineralization, while treatment with a hedgehog antagonist blocked these processes, hinting at possible therapeutic strategies.

RESULTS

Concurrent and irreversible OA-like changes in *Prg4*-null TMJs

OA changes and maladaptive remodeling can occur in the TMJ when mechanical stresses exceed its biomechanical adaptive capacity (Ishizuka et al., 2014; Tanaka et al., 2008a), but little is known as to whether the various TMJ components respond to such pathological

insults in unison or differentially, thus limiting current understanding of TMJ pathogenesis. To this end, we further characterized the OA-like structural and phenotypic changes occurring in articular cartilage and discs in *Prg4*-null mice at different post-natal ages. By 3 months, mutant TMJs displayed obvious OA changes including increased thickness of glenoid fossa roof and articular disc, and the condylar heads were slightly enlarged compared to age-matched controls (Figs. 1A, 1C, respectively). By 6 months of age, osteophyte-like cartilage outgrowths emerged from the central portion of glenoid fossa's articular surface and grew into the upper joint cavity (*ujc*) (Fig. 1D, double arrowhead). Concurrently, there was ectopic chondrogenesis in articular disc, and such excess tissue appeared to articulate with the opposing osteophytes (Fig. 1D, triple arrowhead). By 12 months, OA-like changes became exacerbated and consisted of characteristic pathological changes affecting primarily the anterior half to posterior half of mutant TMJs. The anterior half of glenoid fossa became much thicker, and its surface was largely covered by Safranin-O-stained cartilaginous osteophytes developing from its central and/or peripheral sites (Figs. 1E, 1F, double arrowhead and arrowhead, respectively). In contrast, while the posterior half of glenoid fossa was thicker as well, it displayed also bony tissues rich in vasculature and a thick periosteum-like membranous tissues (*po*) covering the articular surface (Figs. 1G, 1H). The ectopic cartilages forming in the disc were much larger in size by this age (Fig. 1F, triple arrowhead) and a plica -a fold of the synovial membrane- formed between the cartilages protruding from the mesial side of the synovial membrane (Figs. 1E. 1G, arrow). Maladaptive changes were also apparent in the mandibular condyles in *Prg4*-null mice. Micro-CT analysis revealed the characteristic morphological changes and osseous abnormalities in mutant condylar head and neck (Fig. 1J, arrowhead). Sagittal, bird-eye's and frontal views revealed the enlarged condyles along both mesio-lateral and antero-posterior orientations that displayed OA-like changes, including a porous osseous surface (Figs.1L, arrowhead), osteophytes (Fig. 1N, arrowheads) and flattening and concavity (Figs. 1J, 1N, arrowheads) compared to control condyles (Figs. 1I–1M). Calcified tissues were also detected in mesial and lateral aspects of the *Prg4*-null discs and correlated well with development of osteophytes along the condylar periphery (Fig. 1P, arrowheads).

Detailed histomorphometric observations of osteophyte/ectopic cartilage developing in *Prg4*-null TMJs from 3 to 12 months of age revealed that ectopic cartilage and osseous changes occurred first in glenoid fossa and condyle and were preponderant, and were followed by ectopic cartilage formation in the discs (Fig. 1Q). Increased Safranin-O stained articular cartilage and osteophytic lesions in glenoid fossa over age correlated well also with increased roof thickness of the structure (Figs. 1R, 1S).

Molecular and cellular changes in mutant glenoid fossa articular cartilage and chondroid bone and osteophyte formation

Next, we investigated possible developmental mechanisms that could underlie changes in articular cartilage and formation of multiple osteophytes in *Prg4*-null TMJs, including possible distinct osteophyte origin. In wild type mice, upper and lower joint cavities were readily observed in early postnatal stages, and the surface of the bony glenoid fossa/eminence was coated by a thin layer of mesenchymal cells possibly representing presumptive articular cells (*pac*) (Figs. 2A, 2B). With further development, the mesenchymal

tissue became distinguished into four characteristic thin layers (Fig. 2C): a superficial layer (*sf*); a chondroprogenitor layer (*cp*); a chondrocyte layer (*ch*) composed of *Col-I-, Col-II-*, and *Ihh*-expressing chondrocytes (Figs. 2D, 2E, 2F); and chondroid bone (*cb*) entrapping *Col-X*-expressing hypertrophic chondrocytes (Fig. 2G). By 5 months of age, articular cartilage became much thinner and was covered by *Prg4*-expressing superficial cells (Figs. 2H, 2I). In *Prg4* mutants, however, the mesenchymal layer over presumptive glenoid fossa articular cartilage displayed a significantly increased number of mesenchymal cells accompanied by deranged collagen fibril formation in the superficial zone, an important structure critical for mechanical and lubricating function (Ruggiero et. al., 2015) (Fig. 2K) as early as 2 weeks of age. It became even thicker by one month (Fig. 2L) and was composed by *Col I-, Col II-, Col X*- and/or *Ihh*-expressing chondrocytes (Figs. 2M–2P). By 5 month of age, numerous chondrocytes were embedded in the bony mineralized tissue of temporal bone and thus acquired a chondroid bone phenotype. Notably, there were *Sox-9*-expressing chondrogenic cells on the surface (Figs. 2Q–2R).

In long bones, osteophyte formation is closely associated with perichondrium and/or synovial membrane (Bakker et al., 2001; Blaney Davidson et al., 2007; van der Kraan and van den Berg, 2007). Thus, we further investigated osteophyte formation in *Prg4*-null TMJs, paying particular attention to those tissues. Osteophytes developing in the articulating surface of glenoid fossa/eminence did not exhibit obvious fibroblastic cells or periosteum, but appeared to actually initiate from clusters of Safranin-O staining chondrocytes and protruded into the upper joint cavity (ujc) over time (Figs. 3A–3C). At the synovium/articular cartilage junction, the mutant synovial membrane was composed of multiple synovial cells that seemed to extend toward the Safranin-O stained articular cartilage (Figs 3D–3F, 3I, arrow) and formed nodules on the articular cartilage surface (Fig. 3D–3F, arrowhead). *In situ* hybridization analysis of typical makers of synovial membrane revealed that numerous *Col III*-expressing synoviocytes were present in both articular cartilage surface and synovial membrane (Fig. 3G, right panel) compared to controls (Fig. 3G, left panel), and some cells co-expressed *Sox9* indicating that they possess chondrogenic potentials.

Characterization of ectopic cartilage forming in *Prg4*-null TMJs

To characterize ectopic cartilage developing near the glenoid fossa and disc, chondrogenesis, chondrocyte maturation and osteogenesis were evaluated by chondrogenic and osteogenic markers. *Sox9*, *Biglycan (*a small leucine-rich repeat proteoglycan abundant in articular cartilage) (Embree et al., 2010) and *Col-II* displayed specific temporo-spatial expression patters in local chondrogenic and chondrocytic cells (Figs. 4A–4F), indicating that osteophyte-associated chondrocytes were undergoing a typical process of maturation and endochondral bone formation. Similar expression patterns were detected in ectopic cartilage of developing discs (Figs. 4B–4F). *Col-1*, *Bsp* and *Osx* were expressed in osteophytes forming at the glenoid fossa (Figs. 5A, 5C–5F) and articular condyle (Figs. 5J–5L) and in ectopic cartilage at articular disc (Figs. 5G–5I), indicating that the chondrocytes exhibited a secondary chondrocyte phenotype (Beresford, 1981; Hall, 2005). Importantly, numerous TUNEL-positive cells were detectable in the basal side of osteophytes and chondroid bone (Fig. 5B), indicating that local cell death was part of these aberrant processes in mutants.

Hh signaling in osteophytes and its stimulation of chondrogenesis and chondrocyte maturation in glenoid fossa cell cultures

Ihh signaling has important roles in chondrogenesis and endochondral ossification as well as in OA in long bone synovial joints (Lin et al., 2009., Yaeda et al., 2007., Koyama et al., 1996). To determine whether osteophyte formation in mutant TMJs was accompanied by ectopic Hh signaling, we examined expression of *Ihh* and its receptors and *Gli* transcription targets in 6 month-old *Prg4*-null TMJs. Semi-quantitative PCR revealed that *Ihh*, *Ptch1*, *Smoothened* (*Smo*) and *Gli-1, -2 and -3* were all expressed in mutant glenoid fossa/eminence (Fig. 6A). Immunohistochemistry and *in situ* hybridization revealed that *Ihh* and *Gli-1* were preferentially expressed in peripheral cells in developing osteophytes (Figs. 6B, 6C), indicating that Hh signaling had indeed been activated ectopically. Preimmune antibodies generated non-specific background staining (Fig. 6D).

To more directly analyze Hh signaling roles, we tested the responses of glenoid fossa-derived primary cells to Hh treatment. Cells were isolated from 2 month-old wild-type mice and once in monolayer culture, expressed chondrogenic and cartilage markers, thus resembling the expression profile of condylar chondrocytes (Fig. 6E). Treatment with recombinant human SHH (rhSHH) significantly increased alkaline phosphatase (ALP) activity by day 9 over control values (Fig. 6F) and qPCR confirmed the rhSHH-dose dependent enhancement of *Alp* expression (Fig. 6H). rhSHH treatment also stimulated expression of *Col-II* and *Col-X*, markers of chondrocyte differentiation and maturation (Fig. 6I).

To further analyze these responses, we tested the effects of the hedgehog signaling inhibitor HhAntag. To verify its activity, glenoid fossa/eminence explants isolated from 2 month-old *Gli1-nLacZ* hedgehog reporter mice were treated with different concentrations of HhAntag for 4 days. Whole mount *LacZ* staining revealed that HhAntag treatment elicited a dose-dependent decrease of *Gli-1* reporter activity compared to vehicle-treated controls (Figs. 7A–AC). Inhibition of endogenous Hh signaling in articular chondrocytes (*ac*) was further confirmed by histological analysis (Fig. 7D, 7E). To determine whether chondrocyte maturation was counteracted by inhibition of endogenous Hh signaling, glenoid fossa primary cultures were treated continuously with 2 or 5 μM HhAntag. Day 12 cultures displayed a dose-dependent inhibition of APase activity and mineralization as evaluated by Alizarin red staining. qPCR further validated the inhibition of chondrocyte maturation marker expression (Fig. 7I).

DISCUSSION

Here we show that *Prg4*-null TMJs undergo irreversible OA-like changes affecting the major TMJ components - glenoid fossa, articular condyle and articular disc- in unison. Our data indicate that as the osteophytes grow, the roof of the glenoid fossa becomes significantly thicker and flatter, resulting in loss of its characteristic concave shape for accommodation of both condyle and disc. Concurrently, the condyles lose their convex shape, become flatter and larger along the antero-posterior and mesio-lateral axes, and form ectopic bone along their neck seemingly supporting the enlarged condylar heads. In addition, the mutant articular discs lose their configuration and become larger in size so as to accommodate the

enlarged condylar heads over time (Bechtold et al., 2016). Notably, ectopic chondrogenesis takes place, and it appears that the resulting cartilage articulates with osteophytes emerged in glenoid fossa and condyle, implying that the articular disc undergoes a maladaptive response and attempts to stabilize the articulation with the deformed articular cartilage.

It has been proposed that Prg4/lubricin is one of the major synovial fluid constituents contributing to cartilage boundary lubrication (Flannery et al., 1999; Schaefer et al., 2004; Seror et al., 2015). A recent study suggested that Prg4/lubricin interacts with hyaluronic acid and concentrates it on the articular surface, implying that such interaction endows the joint articulation with a low friction coefficient (Bonnevie et al., 2015). Thus, it is reasonable to postulate that the loss of Prg4/lubricin function could severely compromise boundary lubrication and lead to abnormal mechanical stress on articulating surfaces during TMJ function. Our data together with our recent study indicate that ectopic chondrogenesis and osteophyte formation may represent common pathophysiologic steps during TMJ abnormal lubrication circumstances. In line with previously proposed theses (Wu et al., 2001), our data suggest that Ihh and BMP2 are essential components of mechanotransduction mechanisms eliciting ectopic chondrogenesis and osteophyte formation (Bechtold et al., 2016). Further studies are needed to clarify signaling interactions between these and other signaling molecules during TMJ pathologies.

Our data reveal additional and unexpected roles of Prg4 in TMJ articular cartilage development and in formation of glenoid fossa/eminence. Unlike limb synovial joints that largely form during embryogenesis (Decker et al., 2015), the joint cavity of TMJs becomes apparent and fully functional around birth, and formation of articular cartilage and chondroid bone in the glenoid fossa/eminence initiates around 2 weeks of age (Yasuda et al., 2012). Our data indicate that in *Prg4*-null newborn mice in which boundary lubrication is likely defective, TMJ development becomes compromised. In wild-type mice, chondrocytes differentiate amongst *Col I*-expressing mesenchymal cells in presumptive articulating layer over temporal bone, express *Col I* and *Col II* and thus exhibit features of secondary cartilage (Beresford, 1981; Hall, 2005). With time, these chondrocytes undergo endochondral ossification, become entrapped in the intramembranous bony matrix of temporal bone and form chondroid bone. *Prg4*-expressing superficial cells form and cover the articulating surface of secondary cartilage. In *Prg4*-null mice, however, there is excessive chondrogenesis in the presumptive articular layer followed by widespread chondrocyte hypertrophy and endochondral ossification, leading to excess chondroid bone formation and temporal bone thickening. Notably, the articular surface lacks superficial cells but contains *Sox9*-expressing chondroprogenitors and immature chondrocytes instead. It has been reported that secondary cartilage is induced by mechanical stimuli such as those occurring in articulations, sutures and muscle attachment sites (Beresford, 1993; Solem et al., 2011). Our data strongly indicate that deranged friction by the lack of Prg4 action could have induced onset and progression of excessive chondrogenesis at the glenoid fossa/eminence articulation site. Lack of *Prg4*-expressing superficial cells and presence of *Sox9*-expressing cells coupled with abnormal cellular integrity and morphology could thus account for osteophyte formation over time in *Prg4*-null TMJs.

Our data provide insights into the origin of osteophyte and ectopic cartilage and into major steps involved in formation/mineralization in *Prg4*-null TMJs. The data suggest that the osteophytes emerge from distinct locations within the joints including periarticular sites adjacent to hyperplastic synovial membrane and the articulating surface of cartilage. These findings suggest that skeletal progenitor cells of distinct origins are involved in initiation of these skeletal defects. At the articular surface, multiple osteophytes appear to arise from *Sox9*-expressing cells and undergo endochondral ossification while expressing such characteristic chondrocyte markers as *Col II*, *Ihh*, hedgehog receptors/transcriptional activators and *Col X* and osteogenic markers including *Col I*, *Bsp* and *Osterix*. Interestingly, peripheral chondrocytes of the osteophytes highly expressed these markers as well, while chondrocytes located in more central and basal regions expressed them at much lower levels. The data indicate that preferential growth of osteophytes into the upper joint cavity is primarily regulated by peripheral chondrocytes, while other chondrocytes in the osteophytes may undergo senescence or apoptosis (Fig. 5B). Our data indicate that in contrast, synovial mesenchymal cells expressing *Col III*, a major matrix constituent of synovial tissue (Eyre and Muir, 1975; Sandberg and Vuorio, 1987), aggregate at the synovium-cartilage border of the glenoid fossa/eminence and subsequently undergo chondrogenesis in conjunction with *Sox9*-expression. Our findings are in agreement with pathological changes observed in the joints of CACP patients showing synovial hypertrophy and invasion of cartilage surface by synoviocytes that result in severe disruption of joint function (Rhee et al., 2005). Osteophytes/ectopic cartilage arising in mandibular condyles and discs also express secondary cartilage markers. In sum, our observations suggest that regardless of where the chondroprogenitors and chondrocytes originate, the end result is similar: ectopic chondrogenesis and ectopic cartilage/osteophyte formation in *Prg4*-null TMJs, irreversibly hampering TMJ function.

Our in vitro data indicate that primary cells isolated from wild-type glenoid fossa express chondrocyte/osteoblast gene expression profiles similar to those of condylar chondrocytes, indicating that glenoid fossa chondrocytes are able to retain their secondary chondrocyte-characteristics in culture. In primary glenoid fossa cell cultures, we find that rhSHH is a potent stimulator of chondrogenic differentiation as indicated by increases in APase activity and expression of chondrocyte maturation markers. The role of Hh signaling in chondrocyte maturation was validated further by HhAntag treatment that led to marked reductions of APase activity, matrix mineralization and chondrocyte maturation marker expression. We also observed HhAntag-dose dependent reductions of *Gli-1* transcriptional activity in glenoid fossa/eminence explant cultures, indicating that HhAntag interferes with canonical Hh pathway (Mundy et al., 2015). Thus, it appears that the Hh signaling pathway could be targeted to block the initiation and/or progression of ectopic chondrogenesis and ectopic cartilage and osteophyte formation in pathologies such as TMJ osteoarthritis and related conditions.

MATERIALS & METHODS

Transgenic mice

Prg4$^{+/-}$ mutant mice were kindly provided by Dr. Matthew Warman (Boston Children's Hospital, Boston, MA) (Rhee et al., 2005). Animals were maintained in accordance with NIH Guide for Care and Use of Laboratory Animals, and protocols were approved by the IACUC of The Children's Hospital of Philadelphia.

IHH peptide antibody synthesis

A synthetic peptide was synthesized encompassing residues 41–55 of human IHH (CPRKLVPLAYKQFSPN; accession NM_000193), containing an added Cysteine on the N-terminus to facilitate coupling to Maleimide-Activated KLH (Thermo Scientific). The KLH-conjugated peptide was subsequently used to generate polyclonal (IgY) antibodies in chickens. Antibody production was carried out by Cocalico Biologicals (Reamstown, PA).

Histological, immunohistochemical, histomorhometric and *in situ* hybridization analyses

Age matched *Prg4* mutants and wild-type littermates were evaluated at postnatal day 0 (P0, n=6), P14 (2 wks, n=6), 1 months (n=12), 3 months (n=8), 5 months (n=4), 6 months (n=12), and 12 months (n=6) of age. Mice were fixed with 4% paraformaldehyde overnight, decalcified for 2 weeks in 10% EDTA/2% paraformaldehyde (PFA), dehydrated, and embedded in paraffin. For immunohistochemistry, antigen retrieval was performed in citrate buffer (pH 6.0) by boiling for 10 min and then incubating in citrate butter at room temperature for 10 min. Endogenous peroxidase was blocked by incubation with 3% H_2O_2 for 10 min. Sections were treated with PBST/1% BSA for blocking and subsequently incubated with chicken Ihh antibodies (1:50) overnight at 4°C. The sections were washed and then incubated with biotinylated goat anti-chicken secondary antibody, and the signal was visualized using an HRP/DAB detection IHC kit according to the manufacturer's instructions (Abcam Plc.; Cambridge, UK). Companion serial sections were treated with preimmune chicken IgY, which served as negative controls.

For *in situ* hybridization, sections were hybridized with antisense or sense ^{35}S-labeled probes as described in detail previously (Koyama et al., 2007). cDNA clones used as templates for probes included: *Sox9* (nt, 116–856; NM_011448), *Bsp* (nt. 1100–1420; NM_008318); *collagen I* (nt. 233–634; NM_007742); *collagen II* (Col II)(nt.1095–1344; X57982), *collagen X* (nt.1302–1816; NM009925), *Gli1* (nt. 1226–1580; NM_010296); *Osterix* (nt. 40–1727; NM_130458) and *Prg4* (nt. 41–2646; AB034730).

Cell cultures

Cultures were prepared from glenoid fossa/eminence samples isolated from 2 month-old wild-type mice (n=32) as described (Bechtold et al., 2015) with some modifications. Isolated glenoid fossae were incubated with 2.5 U/ml dispase (MP Biomedicals, LLC, Solon, OH) and 600 U/ml (3mg/ml) type I collagenase (Worthington Biochemical Corporation, Lakewood, NJ) in HBSS with Ca^{2+} and Mg^{2+} for 10 min at 37°C with agitation, and then the surface was curetted. Dissociated cells with tissue fragments were cultured together on collagen 1 substrate-coated 6 well culture plates in DMEM containing 10% FBS, 0.1%

Fungizone and antibiotics. Cells were expanded in 6 well culture plates, reared in a higher density to restore native cell characteristics, and passaged three to five times prior to use in experiments. For detection of alkaline phosphatase activity, the cultures were grown for 9 days in DMEM containing 10% FBS, 10 μg/mL ascorbic acid and 10 mM of β-glycerophosphate. Recombinant human Sonic hedgehog protein (rhSHH) was used at concentration of 100–250 ng/ml (R&D Systems; Minneapolis MN) and HhAntag, a hedgehog signaling inhibitor that blocks the activity of the signaling receptor Smoothened (provided as a generous gift from Genentech; San Francisco, CA) was used at a concentration of 2 or 5 μM. For ALP staining, cells were washed three times with TBS, then treated with a solution of 5-bromo-4-chloro-3-indolyl-phosphate and nitro blue tetrazolium (Wako Pure Chemical Industries, Ltd.) for 15 min. For Alizarin red staining, fixed cells were rinsed with water and stained with freshly made Alizarin red staining solution (1% Alizarin red, pH 6.3 adjusted with 0.5% ammonium hydroxide) for 10 min.

For organ culture, glenoid fossae/eminences isolated from 2 month-old *Gli1-nLacZ* mice were cultured for 4 days in complete medium supplemented with 1% FBS in the absence or presence of 100–200 μM HhAntag. Tissues were fixed with 0.2% gluteraldehyde for 15 min on ice, washed, and processed for β–galactosidase staining (EMD Millipore) at 37°C for 4 hrs to overnight.

Quantitative real-time PCR

Quantitative real-time PCR was carried out using SYBR Green PCR Master Mix in an Applied Biosystems 7500 according to manufacture's protocol. *Gapdh* was used as endogenous control, and relative expression was calculated using the ΔΔCT method. For relative mRNA calculation, untreated cultures served as reference for comparison between groups. Data were expressed in arbitrary units.

μCT analysis

Mouse condyles were examined using a viva μCT 40 CT scanner (Scanco Medical AG, Basseldorf, Switzerland), and analyzed using μCT v6.0 vivaCT software. Serial 12.5 μm 2-D and 3-D images were acquired at 70 kV and 113 mA. The raw data from the μCT scans were compiled into 2D gray scale images that were then contoured to define the condyles. Binary images were generated using a threshold of 280. Virtual 3D models were then constructed and analyzed for morphological abnormalities (Laurita et al., 2011).

Statistical analysis

Data were analyzed using two-sided Student's t-test. *p*-values less than 0.05 were considered as statistically significant ($p<0.05$). All statistical data are presented as means ± SD.

Acknowledgments

We thank Dr. Matthew Warman for kindly proving the *Prg4*-null mice. We would like to express our gratitude to Genentech Inc. for providing HhAntag. This study was supported by National Institutes of Health grants (NIDCR grant RO1DE023841 and NIAMS grant RO1AR061758). R.S.D. is the recipient of a postdoctoral training grant (1F32AR064071) from the NIH.

References

Alman BA. The role of hedgehog signalling in skeletal health and disease. Nat Rev Rheumatol. 2015; 11:552–60. [PubMed: 26077918]

Arnett GW, Milam SB, Gottesman L. Progressive mandibular retrusion-idiopathic condylar resorption. Part II. Am J Orthod Dentofacial Orthop. 1996; 110:117–27. [PubMed: 8760837]

Bakker AC, van de Loo FA, van Beuningen HM, Sime P, van Lent PL, van der Kraan PM, Richards CD, van den Berg WB. Overexpression of active TGF-beta-1 in the murine knee joint: evidence for synovial-layer-dependent chondro-osteophyte formation. Osteoarthritis Cartilage. 2001; 9:128–36. [PubMed: 11237660]

Bechtold TE, Saunders C, Mundy C, Um H, Decker RS, Salhab I, Kurio N, Billings PC, Pacifici M, Nah HD, Koyama E. Excess BMP Signaling in Heterotopic Cartilage Forming in Prg4-null TMJ Discs. J Dent Res. 2015

Beresford, WA. Chondroid bone, secondary cartilage and metaplasia. Baltimore, MD, USA: Urban & Schwarzenberg; 1981. p. 23-47.

Beresford, WA. Cranial skeletal tissues: diversity and evolutionary trends. In: Hanken, J.; Hall, BK., editors. The Skull. Chicago: University of Chicago Press; 1993. p. 69-130.

Blaney Davidson EN, Vitters EL, van Beuningen HM, van de Loo FA, van den Berg WB, van der Kraan PM. Resemblance of osteophytes in experimental osteoarthritis to transforming growth factor beta-induced osteophytes: limited role of bone morphogenetic protein in early osteoarthritic osteophyte formation. Arthritis Rheum. 2007; 56:4065–73. [PubMed: 18050218]

Bonnevie ED, Galesso D, Secchieri C, Cohen I, Bonassar LJ. Elastoviscous transitions of articular cartilage reveal a mechanism of synergy between lubricin and hyaluronic Acid. PLoS ONE. 2015; 10(11):e0143415.doi: 10.1371/journal.pone.0143415 [PubMed: 26599797]

Decker RS, Koyama E, Pacifici M. Articular Cartilage: Structural and Developmental Intricacies and Questions. Curr Osteoporos Rep. 2015; 13:407–14. [PubMed: 26408155]

Elsaid KA, Fleming BC, Oksendahl HL, Machan JT, Fadale PD, Hulstyn MJ, Shalvoy R, Jay GD. Decreased lubricin concentrations and markers of joint inflammation in the synovial fluid of patients with anterior cruciate ligament injury. Arthritis Rheum. 2008; 58:1707–15. [PubMed: 18512776]

Elsaid KA, Jay GD, Warman ML, Rhee DK, Chichester CO. Association of articular cartilage degradation and loss of boundary-lubricating ability of synovial fluid following injury and inflammatory arthritis. Arthritis Rheum. 2005; 52:1746–55. [PubMed: 15934070]

Embree MC, Kilts TM, Ono M, Inkson CA, Syed-Picard F, Karsdal MA, Oldberg A, Bi Y, Young MF. Biglycan and fibromodulin have essential roles in regulating chondrogenesis and extracellular matrix turnover in temporomandibular joint osteoarthritis. Am J Pathol. 2010; 176:812–26. [PubMed: 20035055]

Eyre DR, Muir H. Type III collagen: A major constituent of rheumatoid and normal human synovial membrane. Connect Tissue Res. 1975; 4:11–16. [PubMed: 130225]

Flannery CR, Hughes CE, Schumacher BL, Tudor D, Aydelotte MB, Kuettner KE, Caterson B. Articular cartilage superficial zone protein (SZP) is homologous to megakaryocyte stimulating factor precursor and Is a multifunctional proteoglycan with potential growth-promoting, cytoprotective, and lubricating properties in cartilage metabolism. Biochem Biophys Res Commun. 1999; 254:535–41. [PubMed: 9920774]

Flannery CR, Zollner R, Corcoran C, Jones AR, Root A, Rivera-Bermudez MA, Blanchet T, Gleghorn JP, Bonassar LJ, Bendele AM, Morris EA, Glasson SS. Prevention of cartilage degeneration in a rat model of osteoarthritis by intraarticular treatment with recombinant lubricin. Arthritis Rheum. 2009; 60:840–7. [PubMed: 19248108]

Gleghorn JP, Jones AR, Flannery CR, Bonassar LJ. Boundary mode lubrication of articular cartilage by recombinant human lubricin. J Orthop Res. 2009; 27:771–7. [PubMed: 19058183]

Hill A, Duran J, Purcell P. Lubricin protects the temporomandibular joint surfaces from degeneration. PLoS One. 2014; 9:e106497. [PubMed: 25188282]

Hunter A, Kalathingal S. Diagnostic imaging for temporomandibular disorders and orofacial pain. Dent Clin North Am. 2013; 57:405–18. [PubMed: 23809300]

Hussain AM, Packota G, Major PW, Flores-Mir C. Role of different imaging modalities in assessment of temporomandibular joint erosions and osteophytes: a systematic review. Dentomaxillofac Radiol. 2008; 37:63–71. [PubMed: 18239033]

Ishizuka Y, Shibukawa Y, Nagayama M, Decker R, Kinumatsu T, Saito A, Pacifici M, Koyama E. TMJ degeneration in SAMP8 mice is accompanied by deranged Ihh signaling. J Dent Res. 2014; 93:281–7. [PubMed: 24453178]

Jay GD, Britt DE, Cha CJ. Lubricin is a product of megakaryocyte stimulating factor gene expression by human synovial fibroblasts. J Rheumatol. 2000; 27:594–600. [PubMed: 10743795]

Jay GD, Tantravahi U, Britt DE, Barrach HJ, Cha CJ. Homology of lubricin and superficial zone protein (SZP): products of megakaryocyte stimulating factor (MSF) gene expression by human synovial fibroblasts and articular chondrocytes localized to chromosome 1q25. J Orthop Res. 2001; 19:677–87. [PubMed: 11518279]

Koyama E, Leatherman JL, Noji S, Pacifici M. Early chick limb cartilaginous elements possess polarizing activity and express hedgehog-related morphogenetic factors. Dev Dyn. 1996; 207:344–54. [PubMed: 8922533]

Koyama E, Saunders C, Salhab I, Decker RS, Chen I, Um H, Pacifici M, Nah HD. Lubricin is Required for the Structural Integrity and Post-natal Maintenance of TMJ. J Dent Res. 2014; 93:663–670. [PubMed: 24834922]

Koyama E, Young B, Nagayama M, Shibukawa Y, Enomoto-Iwamoto M, Iwamoto M, Maeda Y, Lanske B, Song B, Serra R, Pacifici M. Conditional Kif3a ablation causes abnormal hedgehog signaling topography, growth plate dysfunction, and excessive bone and cartilage formation during mouse skeletogenesis. Development. 2007; 134:2159–69. [PubMed: 17507416]

Laurita J, Koyama E, Chin B, Taylor JA, Lakin GE, Hankenson KD, Bartlett SP, Nah HD. The Muenke syndrome mutation (FgfR3P244R) causes cranial base shortening associated with growth plate dysfunction and premature perichondrial ossification in murine basicranial synchondroses. Dev Dyn. 2011; 240:2584–96. [PubMed: 22016144]

Lin AC, Seeto BL, Bartoszko JM, Khoury MA, Whetstone H, Ho L, Hsu C, Ali SA, Alman BA. Modulating hedgehog signaling can attenuate the severity of osteoarthritis. Nat Med. 2009; 15:1421–5. [PubMed: 19915594]

Maeda Y, Nakamura E, Nguyen MT, Suva LJ, Swain FL, Razzaque MS, Mackem S, Lanske B. Indian Hedgehog produced by postnatal chondrocytes is essential for maintaining a growth plate and trabecular bone. Proc Natl Acad Sci U S A. 2007; 104:6382–7. [PubMed: 17409191]

Marcelino J, Carpten JD, Suwairi WM, Gutierrez OM, Schwartz S, Robbins C, Sood R, Makalowska I, Baxevanis A, Johnstone B, Laxer RM, Zemel L, Kim CA, Herd JK, Ihle J, Williams C, Johnson M, Raman V, Alonso LG, Brunoni D, Gerstein A, Papadopoulos N, Bahabri SA, Trent JM, Warman ML. CACP, encoding a secreted proteoglycan, is mutated in camptodactyly-arthropathy-coxa vara-pericarditis syndrome. Nat Genet. 1999; 23:319–22. [PubMed: 10545950]

Mundy C, Bello A, Sgariglia F, Koyama E, Pacifici M. HhAntag, a Hedgehog Signaling Antagonist, Suppresses Chondrogenesis and Modulates Canonical and Non-Canonical BMP Signaling. J Cell Physiol. 2015

Nitzan DW. 'Friction and adhesive forces'--possible underlying causes for temporomandibular joint internal derangement. Cells Tissues Organs. 2003; 174:6–16. [PubMed: 12784037]

Ochiai T, Shibukawa Y, Nagayama M, Mundy C, Yasuda T, Okabe T, Shimono K, Kanyama M, Hasegawa H, Maeda Y, Lanske B, Pacifici M, Koyama E. Indian hedgehog roles in post-natal TMJ development and organization. J Dent Res. 2010; 89:349–54. [PubMed: 20200412]

Pacifici M, Koyama E, Iwamoto M. Mechanisms of synovial joint and articular cartilage formation: recent advances, but many lingering mysteries. Birth Defects Res C Embryo Today. 2005; 75:237–48. [PubMed: 16187328]

Rando C, Waldron T. TMJ osteoarthritis: a new approach to diagnosis. Am J Phys Anthropol. 2012; 148:45–53. [PubMed: 22371124]

Rhee DK, Marcelino J, Baker M, Gong Y, Smits P, Lefebvre V, Jay GD, Stewart M, Wang H, Warman ML, Carpten JD. The secreted glycoprotein lubricin protects cartilage surfaces and inhibits synovial cell overgrowth. J Clin Invest. 2005; 115:622–31. [PubMed: 15719068]

Ruggiero L, Zimmerman BK, Park M, Han L, Wang L, Burris DL, Lu XL. Roles of the Fibrous Superficial Zone in the Mechanical Behavior of TMJ Condylar Cartilage. Ann Biomed Eng. 2015; 43:2652–62. [PubMed: 25893511]

Sandberg M, Vuorio E. Localization of types I, II, and III collagen mRNAs in developing human skeletal tissues by in situ hybridization. J Cell Biol. 1987; 104:1077–84. [PubMed: 3558480]

Schaefer DB, Wendt D, Moretti M, Jakob M, Jay GD, Heberer M, Martin I. Lubricin reduces cartilage--cartilage integration. Biorheology. 2004; 41:503–8. [PubMed: 15299281]

Schmidt TA, Gastelum NS, Nguyen QT, Schumacher BL, Sah RL. Boundary lubrication of articular cartilage: role of synovial fluid constituents. Arthritis Rheum. 2007; 56:882–91. [PubMed: 17328061]

Scrivani SJ, Keith DA, Kaban LB. Temporomandibular disorders. N Engl J Med. 2008; 359:2693–705. [PubMed: 19092154]

Seror J, Zhu L, Goldberg R, Day AJ, Klein J. Supramolecular synergy in the boundary lubrication of synovial joints. Nat Commun. 2015; 6:6497. [PubMed: 25754223]

Shibukawa Y, Young B, Wu C, Yamada S, Long F, Pacifici M, Koyama E. Temporomandibular joint formation and condyle growth require Indian hedgehog signaling. Dev Dyn. 2007; 236:426–34. [PubMed: 17191253]

Shintaku W, Enciso R, Broussard J, Clark GT. Diagnostic imaging for chronic orofacial pain, maxillofacial osseous and soft tissue pathology and temporomandibular disorders. J Calif Dent Assoc. 2006; 34:633–44. [PubMed: 16967673]

Smith MD. The normal synovium. Open Rheumatol J. 2011; 5:100–6. [PubMed: 22279508]

Solem RC, Eames BF, Tokita M, Schneider RA. Mesenchymal and mechanical mechanisms of secondary cartilage induction. Dev Biol. 2011; 356:28–39. [PubMed: 21600197]

Tanaka E, Detamore MS, Mercuri LG. Degenerative disorders of the temporomandibular joint: etiology, diagnosis, and treatment. J Dent Res. 2008a; 87:296–307. [PubMed: 18362309]

Tanaka E, Detamore MS, Tanimoto K, Kawai N. Lubrication of the temporomandibular joint. Ann Biomed Eng. 2008b; 36:14–29. [PubMed: 17985243]

van der Kraan PM, van den Berg WB. Osteophytes: relevance and biology. Osteoarthritis Cartilage. 2007; 15:237–44. [PubMed: 17204437]

Wu Q, Zhang Y, Chen Q. Indian hedgehog is an essential component of mechanotransduction complex to stimulate chondrocyte proliferation. J Biol Chem. 2001; 276:35290–6. [PubMed: 11466306]

Yasuda T, Nah HD, Laurita J, Kinumatsu T, Shibukawa Y, Shibutani T, Minugh-Purvis N, Pacifici M, Koyama E. Muenke syndrome mutation, FgfR3P(2)(4)(4)R, causes TMJ defects. J Dent Res. 2012; 91:683–9. [PubMed: 22622662]

Zarb GA, Carlsson GE. Temporomandibular disorders: osteoarthritis. J Orofac Pain. 1999; 13:295–306. [PubMed: 10823044]

Highlights

- Prg4-null TMJs exhibit irreversible osteoarthritis-like changes.
- Osteophyte formation in Prg4-null TMJs is associated with ectopic hedgehog signaling.
- Loss of Prg4 function results in abnormal endochondral bone formation in the glenoid fossa.
- Prg4-mediated boundary lubrication is indispensable for TMJ maintenance

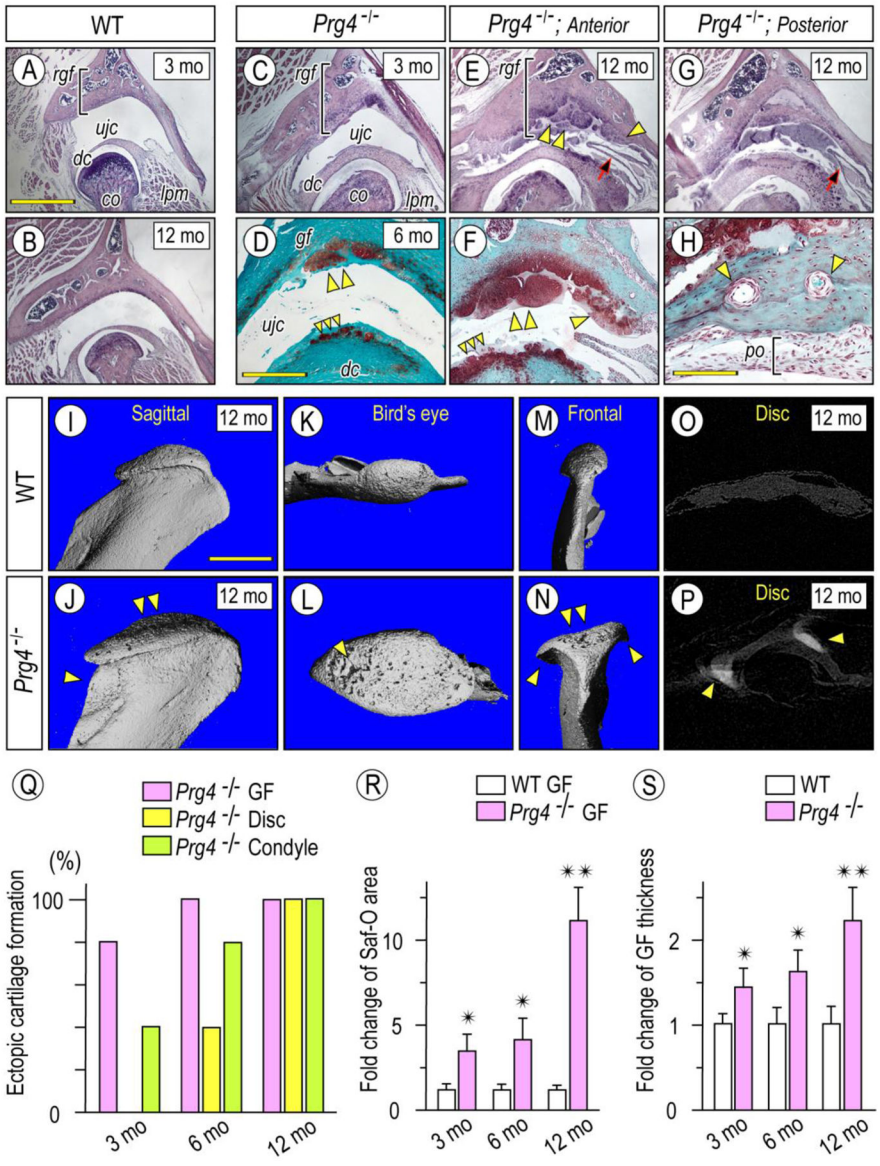

Figure 1. Abnormal cartilage, osteophytes and bone forming in *Prg4*$^{-/-}$ mice

Frontal sections from TMJs prepared from 3 month- (**A, C**), 6 month- (**D**) and 12 month-old (**B, E**–H) control (**A, B**) and *Prg4*$^{-/-}$ (**C**–**H**) mice were processed for Hematoxylin (**A**–**C, E, G**) or Safranin-O/fast green (**D, F, H**) staining. Multiple osteophytes (**D, E, F**; double arrowhead) with preferential growth into the upper joint cavity (*ujc*) in *Prg4*$^{-/-}$ mice resulted in the increased roof of the GF thickness (*rgf*, bracket) and decreased the space of the upper joint cavity (**B** vs **E, G**). Note that osteophyte formation was initiated in 2 distinct sites of the GF/eminence: the articulating surface (double arrowhead in **D–F**) and the synovium/articular cartilage junction (arrowhead in **E, F**). Note also that bone tissue forming in the posterior portion of *Prg4*$^{-/-}$ TMJ was supplied with well-developed nutrient vessels (arrowheads) and coated with periosteum-like tissue (**H**; *po,* bracket) (**H**). 3D microCT images of mandibular condyles from 12 month-old control (**I–O**) and *Prg4*$^{-/-}$ (**J–P**) mice: sagittal (**I, J**), bird's eye (**K, L**) or frontal (**M, N**) view (n=3 for each group). X-ray images

of articular discs from 12 month-old control (**O**) and *Prg4*$^{-/-}$ (**P**) mice and ectopic mineralization detected in mutant disc (**P**; arrowheads). Analysis of serial frontal and parasagittal sections reveals: increased incidence of ectopic cartilage/osteophyte formation in GF, disc and condyle in *Prg4*$^{-/-}$ mice (**Q.** *n*=5 for 3 months and 5 months and *n*=3 for 12 months); fold change of Safranin-O stained area of articular cartilage and osteophytes of glenoid fossa/section (**R,** *n=3* for mouse/each group); and thickness of roof of glenoid fossa (*rgf*) (**S,** indicated by bracket**,** *n=3* for mouse/each group) in *Prg4*$^{-/-}$ mice compared to age-matched control littermates. Areas were randomly selected from 8 sections per sample (*n=3* for mouse/each group, **p* <0.05, ***p* <0.01) and presented as average ±SD. Scale bars: 0.9 mm in **A** for **A**, **B**, **C**, **E**, **G**; 550 μm in **D** for **D, F**; 65 μm in **H;** 1.2 mm for I–P. *gf, glenoid fossa; dc, disc; cd, condyle, ujc, upper joint cavity; po, periosteum; lpm, lateral pterygoid muscle.*

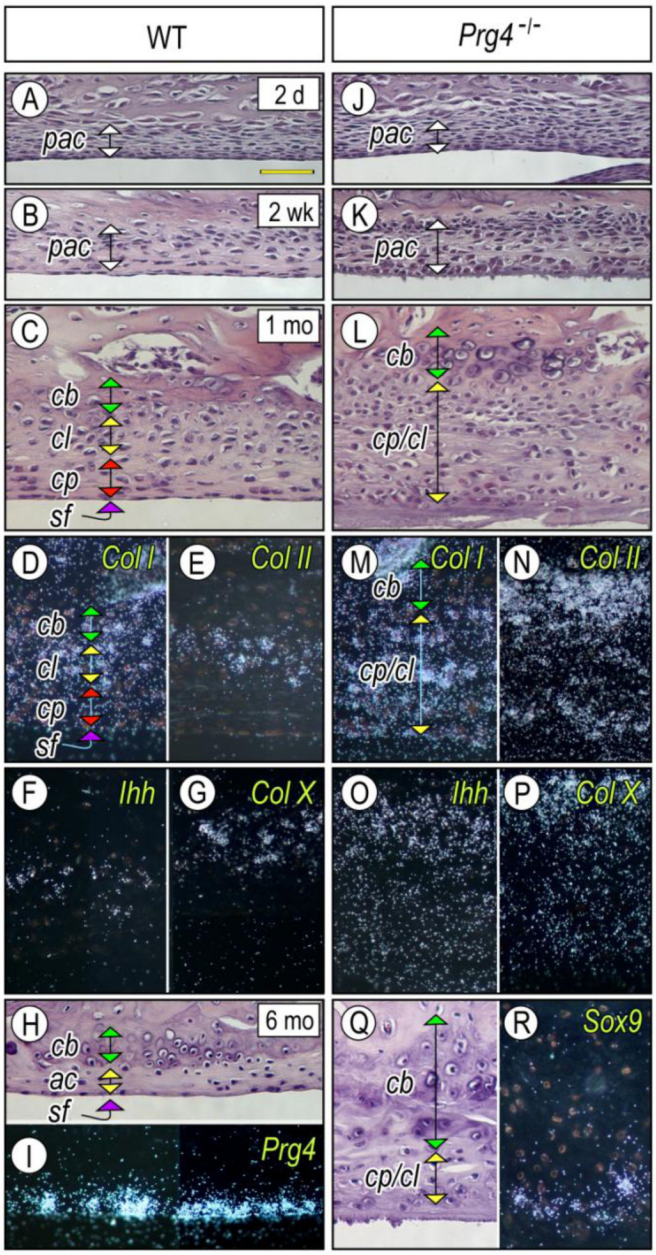

Figure 2. Excessive chondrogenesis and chondroid bone forming in glenoid fossa of *Prg4*-null mice

Parasagittal sections prepared from TMJs of 2 day- (**A, J**), 2 week- (**B, K**), 1 month- (**C–G, L–P**) and 5 month-old (**H, I, Q, R**) control (**A–I**) and *Prg4*$^{-/-}$ (**J–R**) mice were stained with Hematoxylin & Eosin (**A–C, H–L, Q**). Note that the thickened presumptive articular cartilage layer (*pac*) (**K**) resulted in the expansion of the chondrocyte progenitor layer (*cp*), chondrocyte layer (*cl*) and chondroid bone zone (*cb*) in *Prg4*$^{-/-}$ TMJs (**L, Q**) compared to controls (**C, H**). Sections were processed for *in situ* hybridization with isotope-labeled riboprobes for *Col Iα2* (**D, M**), *Col IIα1* (**E, N**), *Ihh* (**F, O**). *Col X* (**G, P**), *Prg4* (**I**) and *Sox9* (**R**). Scale bar: 55 μm in **A** for **A–R**.

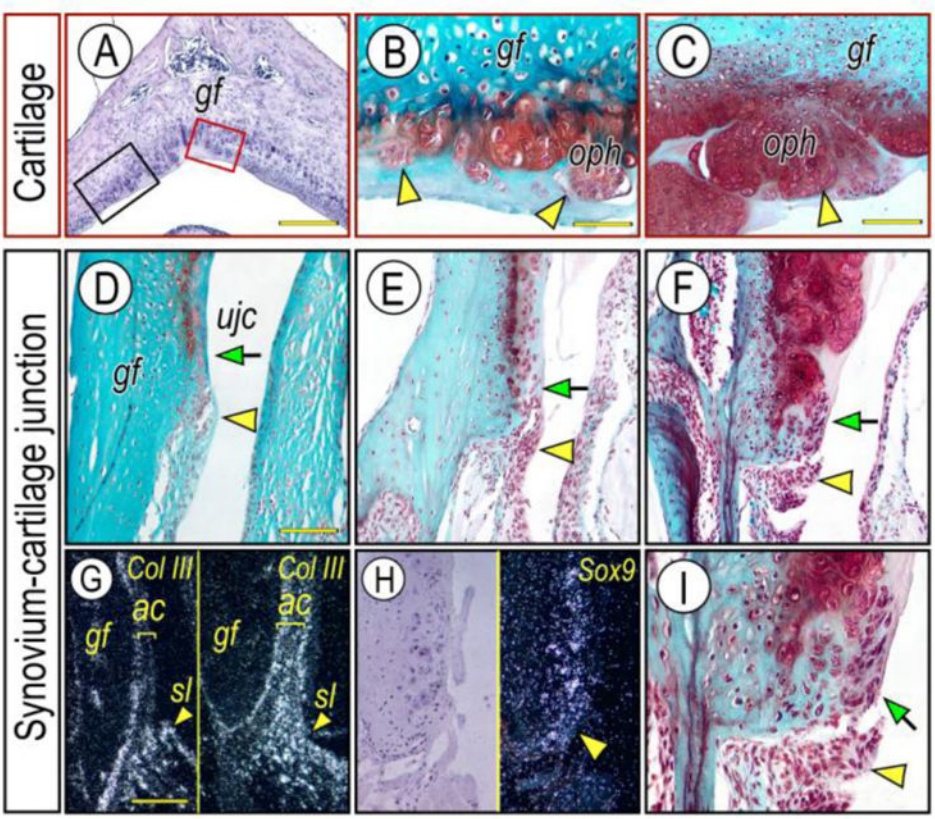

Figure 3. Major steps of osteophyte development near articulating cartilage and synovium-articular cartilage junction in *Prg4*$^{-/-}$ glenoid fossa

Frontal sections prepared from TMJs of 3 month- (**D; G**, right panel), 6-month- (**A, B, E**), 10 month- (**C, F, I**) old *Prg4*$^{-/-}$ mice were stained with Hematoxylin & Eosin (**A**) and Safranin-O (**B–F, I**). Osteophyte development was investigated in red box area (articular cartilage) or black box area (synovium-cartilage junction) of the glenoid fossa (**A)** representing the articulating cartilage and synovium-articular cartilage junction, respectively. Note that multiple osteophyte-like chondrocyte clusters start forming in the articulating cartilage surface (**B**, arrowheads), and grow into osteophytes (*oph*) (**C**, arrowhead). Synovial cell mass (**D–F**; arrowhead) present at the synovium-articular cartilage junction before chondrocyte differentiation indicated by lack of Safranin-O staining and its integration into the developing osteophytes (**F, I,** arrow) in the advanced OA condition. Synovium-articular cartilage junction in **F** was magnified to reveal the synovial cell mass (**I,** arrowhead) and integration of synovial cells into developing cartilage/osteophyte (**I,** arrow). *In situ* hybridization with isotope-labeled RNA probe of *type III collagen* (*Col-III*) (**G,** left panel, control; right panel, mutant) and *Sox9* (**H**). Note that *Col-III* transcripts are abundant in the synovial membrane and are much less at the articular cartilage surface, while a numerous number of *Col-III*-expressing cells are detectable in the *Prg4*$^{-/-}$ glenoid fossa. *Sox-9* expressing chondroprogenitor cells detected in the synovium-articular cartilage junction in *Prg4*$^{-/-}$ glenoid fossa. Scale bars: 150 μm in **A**; 45 μm in **B** for **B**, **I;** 80 μm in **C** for **C–F**; 125 μm in **G** for **G–H**. *gf, glenoid fossa; ujc, upper joint cavity; oph, osteophyte; sl, synovial lining cell; ac, articular cartilage.*

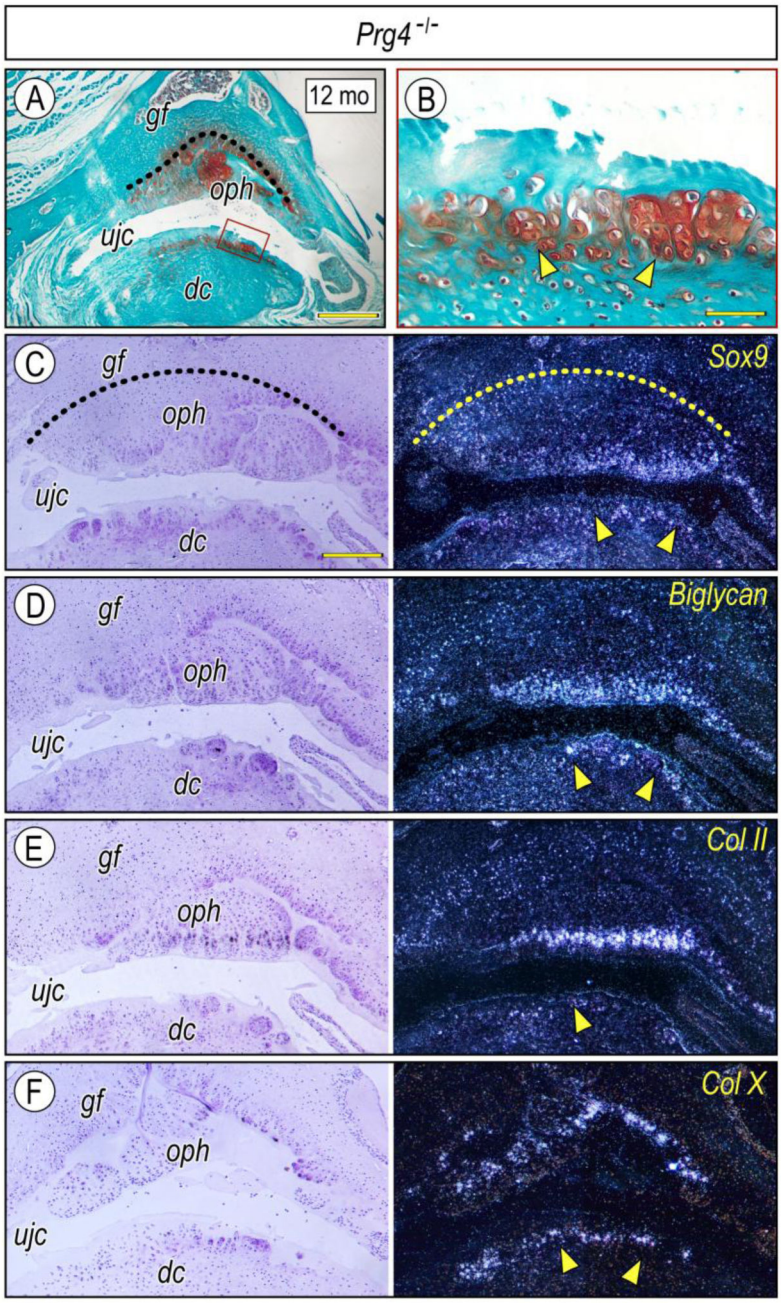

Figure 4. Expression of chondrogenic markers in osteophytes and extopic cartilage developing in *Prg4-null* mice

Frontal sections prepared from TMJs of 12 month-*Prg4-null* mice were stained with Safranin-O (**A, B**). The glenoid fossa articular cartilage is defined by a dashed line to clarify the developing osteophytes (**A, C**). Ectopic cartilage forming at the surface of the articular disc articulating with osteophytes (**A**, boxed area) enlarged in **B**. Serial sections were processed for *in situ* hybridization with isotope-labeled riboprobes for *Sox9* (**C**), *Biglycan* (**D**), *Col IIα1* (**E**) and *Col X* (**F**). Note intense labeling of *Sox9*, *Biglycan*, and *Col IIα1* transcripts, detected in the peripheral chondrocytes of the osteophytes, indicating

preferential growth of the osteophyte into the upper joint cavity (*ujc*). Note also *Col X* expression in the relatively deep region of the cartilage (arrowhead). Scale bars: 250 μm in **A**; 45 μm in **B**; 125 μm in **C** for **C–F**. *gf, glenoid fossa; ujc, upper joint cavity; dc, disc; oph, osteophyte.*

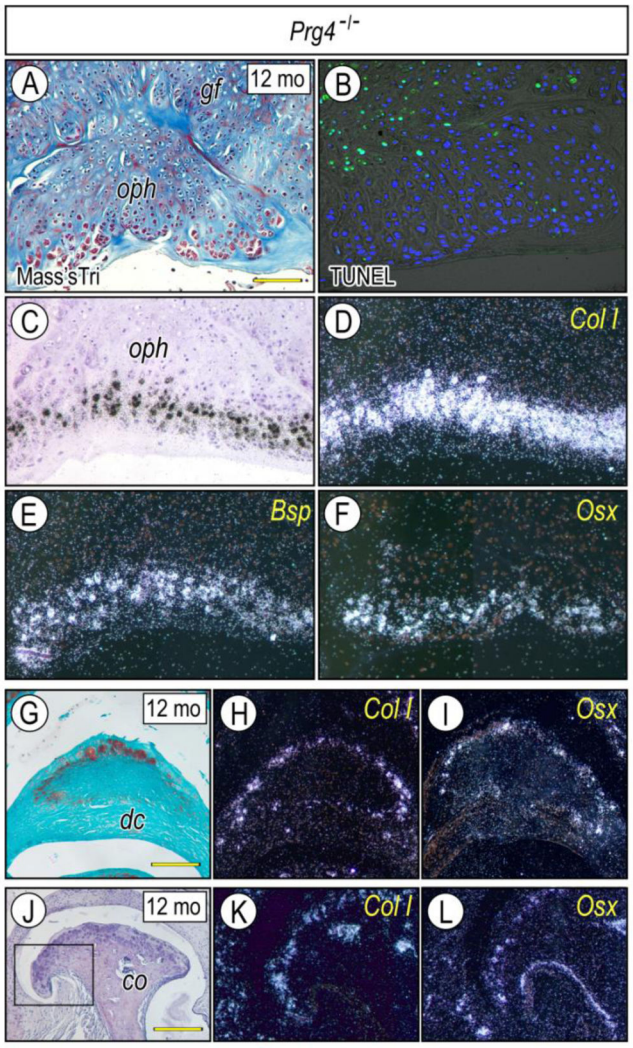

Figure 5. Expression of osteogenic markers in osteophytes and/or ectopic cartilage developing in glenoid fossa, articular disc and mandibular condyle of *Prg4*-null mice

Frontal sections were prepared from TMJs of 12 month-*Prg4*-null mice and stained with Masson's trichrome (**A**), Safranin-O (**G**) and Hematoxylin (**J**) and processed for TUNEL to detect apoptosis (**B**). Serial sections were also processed for *in situ* hybridization with isotope-labeled riboprobes for *Col Iα2* (**D, H, K**), *Bone sialoprotein* (**E**) and *Osterix* (**F, I, L**) in osteophytes (*oph*) forming in the glenoid fossa (*gf*) (**A–F**) and mandibular condyle (*co*) (**J–L**) and ectopic cartilage forming the articular disc (*dc*) (**G–I**). Note intense expression of osteogenic markers at the peripheral region of osteophytes resembling that of chondrogenic markers (Fig. 4), a characteristic feature of seconday cartilage. Boxed area in **J** was enlarged in **K** and **L**. Scale bars: 55 μm in **A** for **A–F**; 80 μm in **G** for **G–I, K–L;** 250 μm in **J**. *gf, glenoid fossa; ujc, upper joint cavity; dc, disc; oph, osteophyte; co, condyle.*

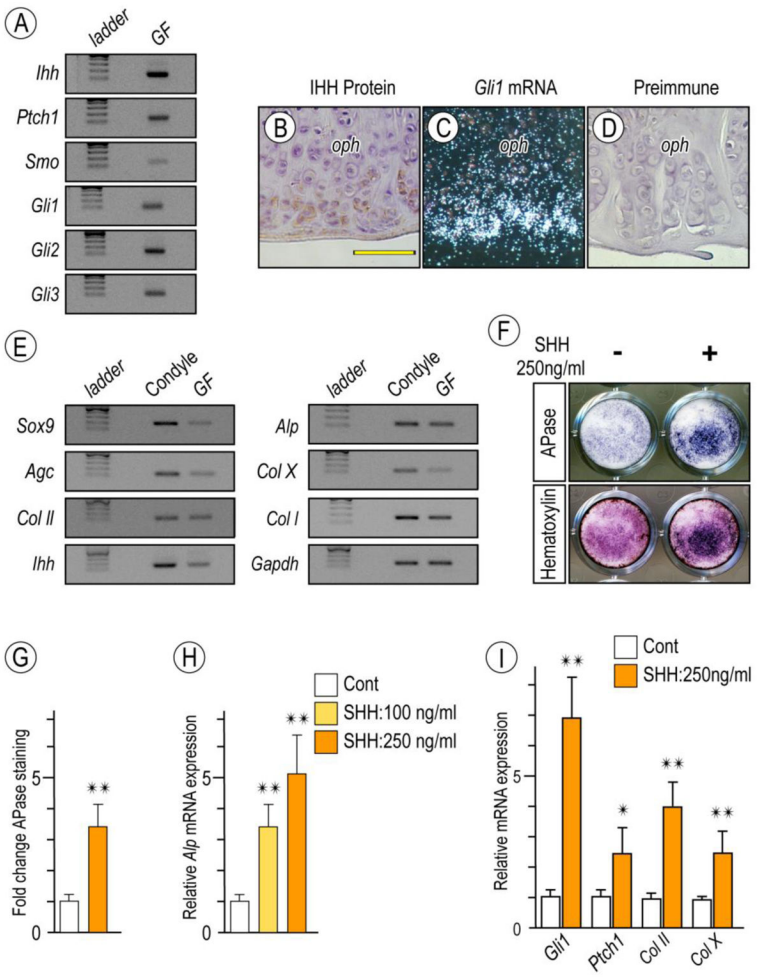

Figure 6. Detection of Hh signaling in osteoarthritic TMJs in *Prg4*-null glenoid fossa and Hh-induced stimulatory effect on chondrocyte maturation by primary glenoid fossa cells

Semi-quantitative PCR analysis of expression of Ihh and its signaling associated molecules in glenoid fossae (GF)/eminences from 6-month-old *Prg4*-null mice (**A**). IHH protein expression by Immunohistochemistry (**B**) and *Gli-1* expression by *in situ* hybridization (**C**) detected at the peripheral region of the osteophytes developing in the glenoid fossa. Sections treated with preimmune chicken IgY served as controls (**D**). Semi-quantitative PCR analysis of expression of chondrocyte markers in mandibular chondyle and glenoid fossa (GF) (**E**). Primary gleniod fossa cells were cultured on 24-well plates and stimulated with rhSHH protein (250ng/ml) for 9 days, fixed, and processed for Alkaline phosphatase activity (**F**; upper panel). Cultures were also counterstained with Hematoxylin to reveal the presence of cells in cultures (**F**; lower panel). Integrated density of Alkaline phosphatase (APase)-stained cultures was measured by ImageJ (**G;** $n=3$, $*p<0.05$). Untreated cultures served as reference for comparison between groups. The data are expressed in arbitrary units. Histograms depicting rhSHH-dose dependent activation of *Alkaline phosphatase* (*Alp*) mRNA (**H**) and increased Hh-transcriptional targets and chondrocyte maturation marker (I) in day 9 primary gleniod fossa cell culture compared to controls ($*p<0.05$, $**p<0.02$). Scale bars: 55 μm in **B** for **B–D**. *oph, osteophyte.*

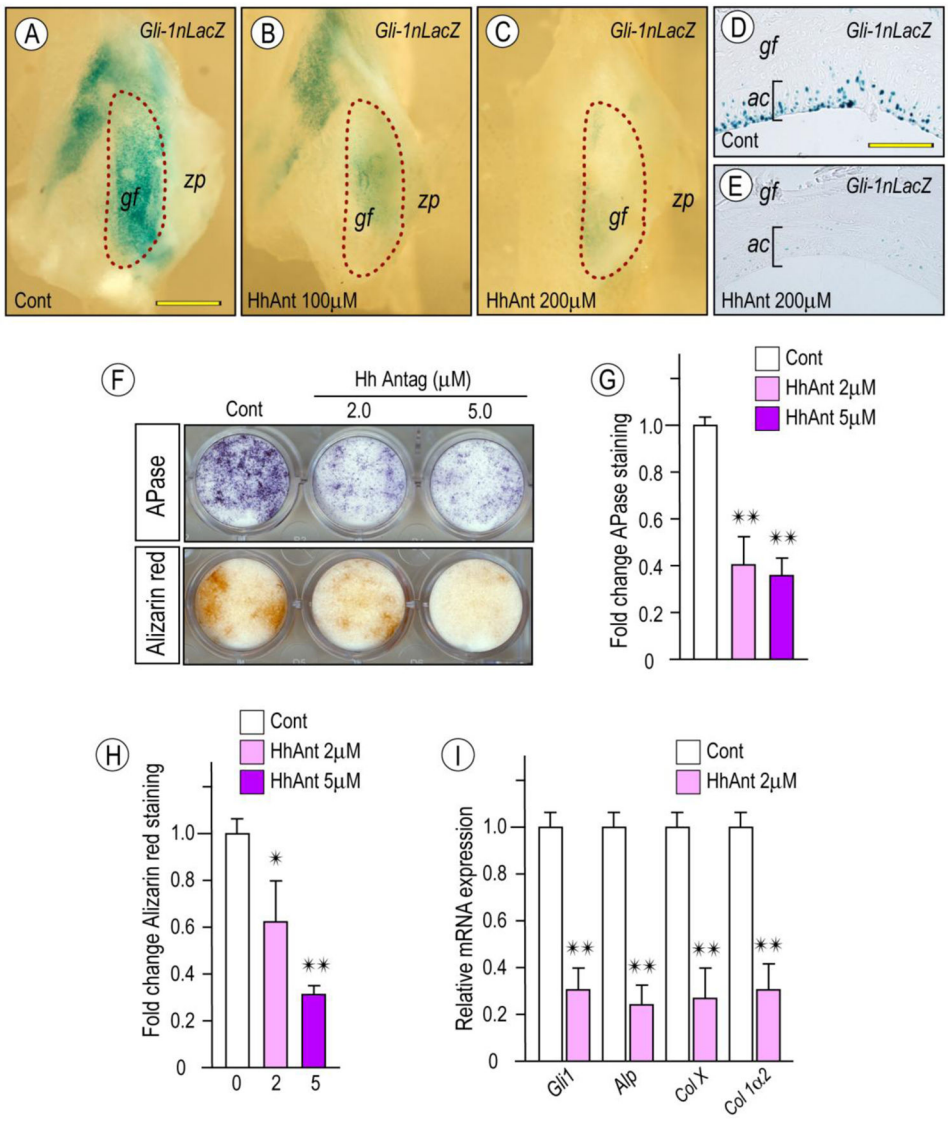

Figure 7. Inhibition of Hh signaling attenuates *Gli-1nLacZ* reporter activity in glenoid fossa/eminence tissues and chondrocyte maturation in primary glenoid fossa cells

Glenoid fossa/eminence from 2 month-old-*Gli1-nLacZ* reporter mice were culture in the presence of HhAntag at indicated concentrations (**B, C**) or control vehicle (**A**), processed for whole-mount LacZ staining (**A–C**) and subsequent sectioning (**D, E**). Note decreased LacZ activity in the articular cartilage of glenoid fossa/eminence treated with HhAntag vs control (**D, E**; respectively). Primary glenoid fossa cells were cultured on 24-well plates and treated with HhAntag at indicated concentrations or control vehicle for 9 days, fixed, and processed for Alkaline phosphatase activity (**F**, top panel) or Alizarin red staining (**F**, lower panel). Integrated density of Alkaline phosphatase-staining (**G**) and Alizarin red-staining (**H**) were quantified by ImageJ (**G;** $n=3$, $*p<0.05$, $**p<0.02$). Untreated cultures served as reference for comparison between groups. The data are expressed in arbitrary units. Histograms depicting HhAntag-dose dependent decrease of Hh signaling molecules and chondrocyte maturation markers in day 9 primary glenoid fossa cell culture compared to controls (**p

<0.02). Scale bars: 2.4 mm in **A** for **A–C**; 80 μm in **D** for **D–E**. *gf, glenoid fossa; zp, zygomatic process; ac, articular cartilage.*